

# Optimal Color Multiplexing for Low-Cost Structured Light 3D Capture System with Two Projectors

Yang Lei, HP Labs, Palo Alto, CA USA

Jan P. Allebach, Purdue University, West Lafayette, IN USA

## Abstract

3D shape reconstruction is one of the most important topics in computer vision and the foundation for a wide field of application. Among various technologies, structured light is one of the most reliable techniques. However, given the field of view of projectors and cameras available in the market, the working distance needed for projectors is typically larger than that for cameras. To reduce the working distance of the projectors while covering the whole working platform, two projectors with their field of view overlapping are used to cover the working area which holds objects to be scanned. We present a spectral analysis based model for the projector-camera system, in order to find the most distinguishable colors for two projectors, and best separate the projected patterns from two projectors. The optimal values of the two colors are determined by the pattern search method in the presence of noise, which is modeled as multivariate Gaussian noise, and characterized for different input colors. The camera sensors' responses to the projector are measured after linearization with gray balance curves. After being properly calibrated, based on one image shot of the object with binary M-array patterns projected on it, the system can reconstruct a 3D shape of the object surface.

## Introduction

3D object reconstruction is becoming an increasingly important research area in both computer vision and image processing, due to its wide application in various fields. Examples include industrial part modeling and inspection, robot navigation, and 3D map-building. Depending on whether the sensing system needs to touch the object or not, there are two types of 3D capture technologies: contact methods and non-contact methods.

Contact 3D capture methods probe the subject through physical touch and record the shape data at the same time. The modern coordinate-measuring machine (CMM) is an example. The machine records the displacement of a probe tip as it slides across a solid surface. CMM is used in manufacturing most of the time for its high accuracy in measurement. However, as with all other products using contact methods, it may cause modifications or even damage to the object, which we would not like to see in some cases, such as when scanning historical artifacts. Another disadvantage of such methods is the slow operation, since it needs to get the shape information point by point.

On the other hand, as a large group of 3D capture techniques, non-contact methods get the shape data of objects without physically touching them. They either rely entirely on ambient light (passive methods) or emit certain controlled radiation or light and detect its reflection (active methods) to probe an object or the environment. For active methods, there are various systems with

different radiation sources or philosophies of measurement, such as time-of-flight, laser scanning, and structured light. On the other hand, passive methods employ the theory of stereo vision, such as stereoscopic systems. Our goal is to accurately capture the 3D shape and color information of everyday small objects and documents at high speed, while using low-cost hardware, such as mobile phone cameras.

Time-of-flight systems are well known for their video rate processing speed. However, their low resolution and the random noise of the sensor have impeded their application for everyday small objects. Recently, an algorithm was proposed to obtain 3D scans of reasonable quality with a sensor that produces low quality data [3]. This algorithm is based on a new combination of a 3D super-resolution method with a probabilistic scan alignment approach that explicitly takes into account the noise characteristics of the sensor. However, the algorithm fails to capture accurate data for certain surface materials, such as highly specular objects. Currently, the super-resolution step takes almost 95% of the runtime, which is too much for low-cost consumer applications.

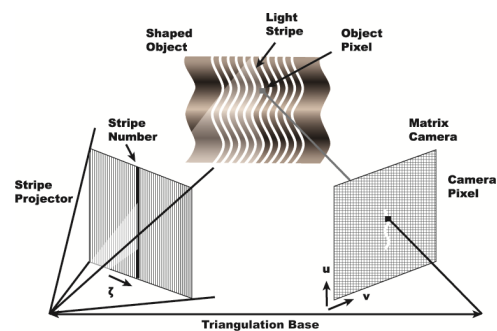


Figure 1: The triangulation principle of a structured light system.

Another large group of 3D-capture techniques is based on triangulation [6], as shown in Fig. 1. Examples include stereoscopic systems, laser scanning systems, and structured light systems [2]. Laser scanning methods shine a laser dot or line on the object and exploit a camera to look for the location of the laser dot/line. In the case of a laser dot, its location in the camera's field of view can be used to determine the 3D location of the point on the object. In some sense, such single-point scanning methods can be seen as the optical equivalent of coordinate measuring machines (CMM), and just as with CMM, it is a painstakingly slow process. With the development of low-cost, high-quality CCD arrays in the 1980s, we can use a laser projector to create a single planar sheet of light and sweep it across the surface of the object. The depth is recovered by the intersection of this plane with the set of lines passing through the 3D stripe on the surface and the camera's center of projection. Effectively removing one dimension of

the raster scan, the swept-plane laser scanning remains a popular solution for rapid shape acquisition. A variety of commercial products use such scanning method, such as the NextEngine 3D Scanner<sup>1</sup>.

With the goal of capturing 3D data from one camera shot, we build a low cost compact structured light system with two projectors and one camera, and project two M-array patterns to the working platform at the same time [7]. Since the system is designed to work with objects whose heights are no larger than 2 inches, and the area that each projector could cover gets smaller as the height of object surface increases, the two projectors are positioned such that their fields of view overlap on the working platform at zero object height. If we use the same color for both patterns, it is impossible to separate them in the overlapped region, since the symbols change their shape when overlapped with each other.

Therefore, we propose to use two different colors for the two patterns. Here comes the problem of choosing which colors we should project so that they can be separated easier. Based on those ideas, we build a color multiplexed camera-projector imaging system model in the presence of multivariate Gaussian noise.

First of all, we measure the color and noise characteristics of the camera-projector imaging system. For the color characterization, we gray balance the camera first, then the camera sensors responses matrix  $A$  to the projector's input are approximated by linear regression on measurements of 27 colors. We assume the noise has zero mean and is uniformly distributed across the camera's field of view. But the noise covariance matrix is color dependent. Using the same 27 colors, we gray balance the camera's response to them first, then calculate the covariance matrix among the red, green, and blue channels for each color. This provides us with 27 noise covariance matrices. For colors other than the 27 we used, their noise covariance matrices are obtained by using trilinear interpolation of the known covariance matrices element by element.

After obtaining system parameters for the model, we define the optimization problem that will find the best input colors. The goal of the optimization problem is to minimize the probability of making a wrong decision about the color in the presence of noise, with the maximum likelihood method being used for classification. The cost function is calculated by numerical integration. The pattern search method [5] is used to find the optimal solution. A validation procedure is recommended to check the optimal solution that has been obtained.

The rest of this paper is organized as follows. In the next section, we describe the design of our dual-projector structured light 3D reconstruction system, followed by a section illustrating the structure of the color multiplexed system model, and the spectral analysis for the camera-projector imaging system. Then we show the imaging system color and noise characterization process and results, which provide parameters for the color multiplexed system model. An optimization problem is then defined to solve for the best input colors. And the procedures to validate a solution to the optimization problem are also presented. At the end, we have the conclusions and future work is summarized.

## Dual-projector Structured-light 3D Capture System Design

Most of the 3D capture products currently in the market have high accuracy, but also are too expensive for object capture of home by hobbyists and small businesses. The goal of designing a low-cost structured light 3D capture system is to maintain sufficient accuracy while keeping the system cost within a range that is suitable for home and small business use. A number of factors, such as resolution, light-level output, geometric distortion, and working distances for the projector, need to be considered.

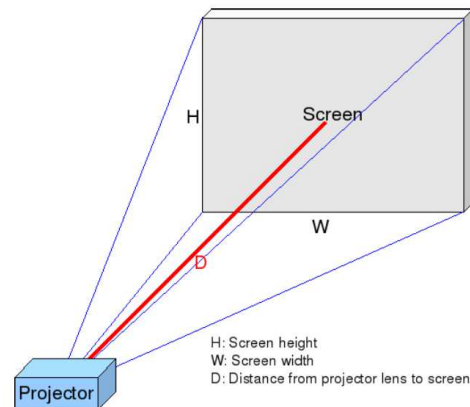


Figure 2: Illustration of throw ratio and throw distance [4].

Almost any digital projector can be used in a 3D structured light system. At least a VGA projector ( $640 \times 480$ ) is recommended. The resolution of the camera should be higher than that of the projector. The projector's throw ratio is the ratio between the throw distance and the width of the screen, where the throw distance is the distance from the screen to the projector. Figure 2 illustrates the throw ratio and throw distance.

In this section, we will describe our prototype system built with the HP TopShot LaserJet Pro M275<sup>2</sup> and two 3M MPro 150 VGA ( $640 \times 480$ ) pocket projectors<sup>3</sup>.

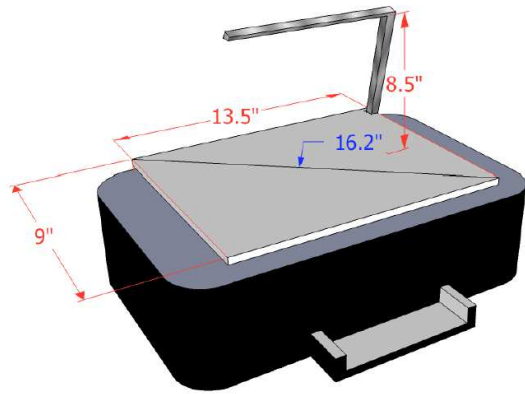
Given the dimensions of the TopShot unit shown in Fig. 3a, for which the width of the platen is 13.5" and the height of the arm containing the camera and light sources is 8.5" above the platen, a projector that has throw ratio =  $\frac{8.5''}{13.5''} \approx 0.63$  would be required. Most projectors on the market are designed to have a relatively large throw ratio. Therefore, given a desired projected image size, the large throw ratio requires a large throw distance, which makes the whole 3D capture system not compact. To solve this issue, Dong [4] introduced a dual projector system, which uses two relatively short-throw-ratio projectors to each cover half of the platen. A model of this design is shown in Fig. 3b. Two heavy-duty posts are used to hold the projectors and control their movement. The final system that was built is shown in Fig. 4. One potential application of this capture system is paper flattening [8].

The dual-projector design is used to reduce the working distance of the projectors while covering the whole working platform, therefore making the system more compact. Two new M-array patterns are designed for the two projectors. The strategy to choose the most separable colors based on the characteristics of the imaging system is illustrated in detail in the rest of this paper.

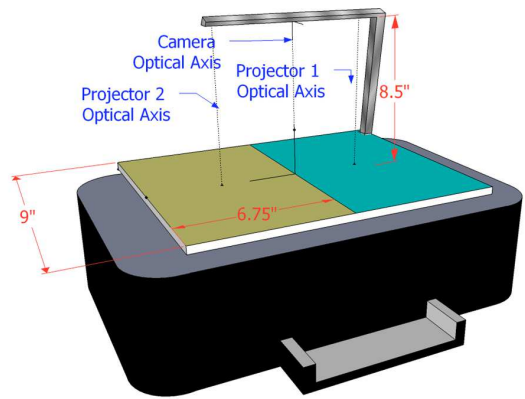
<sup>1</sup>NextEngine Inc. Santa Monica, CA 90401

<sup>2</sup>HP Inc. Palo Alto, CA 94304

<sup>3</sup>3M Company, Saint Paul, MN 55144



(a)



(b)

Figure 3: (a) Required throw ratio given the dimensions of TopShot if only one projector is used. (b) Conceptual design of the dual-projector system built around TopShot. [4].

### Color Multiplexed Imaging System Model

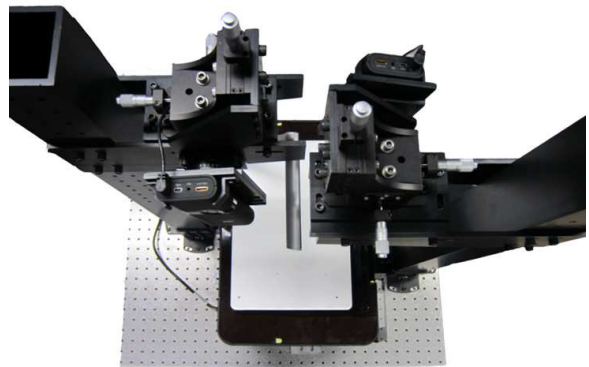
The block diagram in Fig. 5 summarizes the color multiplexed camera-projector imaging system model with multivariate Gaussian noise. In this block diagram, the upper and lower branches show the practical and ideal cases, respectively. At each pixel, the projector's input  $\vec{p}$  could be one of the three following colors: black  $\vec{p}_0 = \vec{0}$ , color 1  $\vec{p}_1$ , and color 2  $\vec{p}_2$ . After linearization, the camera's response vector  $\vec{c}$  to the projector's input could be modeled by a  $3 \times 3$  matrix  $A$ , that is  $\vec{c} = A\vec{p}$ . The spectral analysis based method to calculate matrix  $A$  will be described later in this section.

$\vec{c}$  actually has four possible values at each pixel of the camera. They are response to black  $\vec{c}_0 = \vec{0}$ , response to input color 1  $\vec{c}_1$ , response to input color 2  $\vec{c}_2$ , and response to the overlapped region of color 1 and color 2  $\vec{c}_3 = \vec{c}_1 + \vec{c}_2$ . For each pixel, we need to make a decision among the four cases to determine which pattern it belongs to. The maximum likelihood method is used for the decision making process.

In practice, the imaging system has noise. We model it as zero-mean multivariate Gaussian noise; and the covariance matrix is color dependent. Therefore, the camera response we get is the ideal response  $\vec{c}$  plus the noise  $\vec{n}_{\vec{c}}$ . We call the actual data point  $\vec{c}' = \vec{c} + \vec{n}_{\vec{c}}$ . Finally, the maximum likelihood method is used to make the decision, and generate the output  $o$ .



(a) Side view of the current system.



(b) Top view of the current system.

Figure 4: Latest system setup [4].

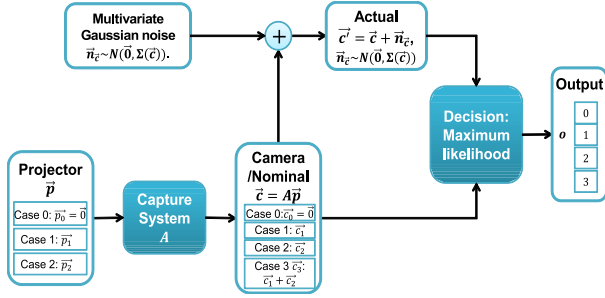


Figure 5: Block diagram for the projector-camera imaging system model.

### System Spectral Analysis

In this subsection, we illustrate the relationship between the projector's input and the camera's response to the projector's corresponding output [1].

Assuming we have the camera's spectral response functions  $Q_R(\lambda)$ ,  $Q_G(\lambda)$ , and  $Q_B(\lambda)$  for the red, green, and blue channels, respectively, The camera's response to a stimulus  $S(\lambda)$  can be calculated by Eqs. 1-3.

$$R_S = \int S(\lambda) Q_R(\lambda) d\lambda. \quad (1)$$

$$G_S = \int S(\lambda) Q_G(\lambda) d\lambda. \quad (2)$$

$$B_S = \int S(\lambda) Q_B(\lambda) d\lambda. \quad (3)$$

Given the projector's spectral density functions  $P_R(\lambda)$ ,  $P_G(\lambda)$ , and  $P_B(\lambda)$ , and the corresponding primary amounts sent to the projector  $p_R$ ,  $p_G$ , and  $p_B$ , the projector's output can be calculated by Eq. 4.

$$P(\lambda) = p_R P_R(\lambda) + p_G P_G(\lambda) + p_B P_B(\lambda). \quad (4)$$

In the camera-projector imaging system we have, the camera's response to the projector's output can be calculated by Eqs. 5-7.

$$R_p = \int (p_R P_R(\lambda) + p_G P_G(\lambda) + p_B P_B(\lambda)) Q_R(\lambda) d\lambda. \quad (5)$$

$$G_p = \int (p_R P_R(\lambda) + p_G P_G(\lambda) + p_B P_B(\lambda)) Q_G(\lambda) d\lambda. \quad (6)$$

$$B_p = \int (p_R P_R(\lambda) + p_G P_G(\lambda) + p_B P_B(\lambda)) Q_B(\lambda) d\lambda. \quad (7)$$

Let  $\vec{c}_p = [R_p, G_p, B_p]^T$ ,  $\vec{p} = [p_R, p_G, p_B]^T$  represent the camera's RGB response values and the projector's input RGB values, respectively. Their relationship can be determined as in Eq. 8.

$$\vec{c}_p = A \vec{p}, \quad (8)$$

where  $A = [a_{ij}]$ , and  $a_{ij} = \int P_j(\lambda) Q_i(\lambda) d\lambda$ ,  $i, j = R, G, B$ .

### System Color and Noise Characterization

The color multiplexed imaging system model presented in the previous section has two sets of parameters to be determined, the camera's response matrix to the projector, and the color dependent covariance matrix for the multivariate Gaussian noise. We refer to them as the system color and noise characteristics, respectively.

For the color and noise measurements we do in this section, the same camera exposure settings and image region are used throughout the process. The camera exposure is set such that when projecting white from both projectors, each RGB channel won't be over-saturated. That is, for each channel, there are fewer than 1% of the pixels that have the value 255. A  $50 \times 55$  image patch in the overlapped region is used for the measurements. The measurement location is shown in Fig. 6.

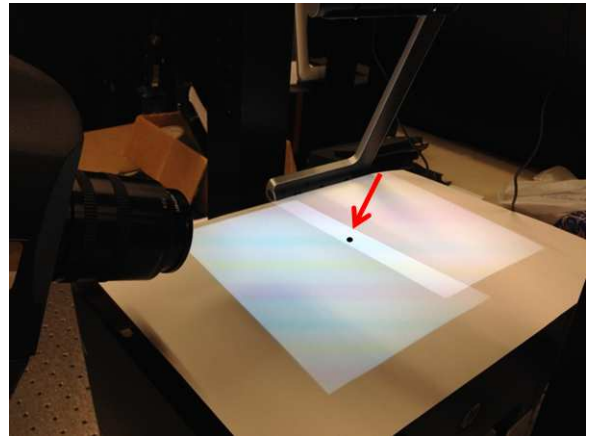


Figure 6: The location of the image patch we measured are marked by a black dot.

### System Color Characterization

#### Camera Gray Balancing

The block diagram in Fig. 7 shows the concept of performing camera gray balancing. 20 different levels of gray images are used for the measurement. The same gray image is projected from both projectors at the same time. Each time we project a different gray image, the Photo Research SpectraScan 705 is used to measure the CIE XYZ values at the location shown in Fig. 6. The CIE Y value is used as luminance value for the red, green, and blue channels. At the same time, we capture an image with the TopShot camera, and compute the average pixel value of the same measured location for the red, green, and blue channel separately. In this way, we have 20 pairs of values for each channel. They are shown as dots in the two-dimensional plots in Fig. 8.

Note that the camera's response to different luminance levels looks linear. This is because we are capturing the raw output from the camera. So we fit those data points with a first order polynomial  $Y_i = aV_i + b$ ,  $i = R, G, B$ , where  $Y_i$  is the CIE Y luminance and  $V_i$  is the corresponding average pixel value of the camera image. The camera gray balance curves and fitting parameters for the red, green, and blue channels are shown in Fig. 8.

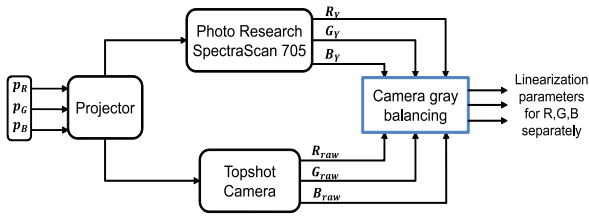


Figure 7: Block diagram for the projector-camera imaging system color characterization.

### Measure the Camera's Response Matrix to the Projector's Input

The block diagram in Fig. 9 shows the concept for measuring the camera's response matrix to the projector's input.

For each projector's input  $\vec{p}$ , we have the camera's raw output  $\vec{c}_{raw}$ . Using the gray balancing result in Fig. 8, we can get the corrected camera's output  $\vec{c}$ . With one pair of  $\vec{p}$  and  $\vec{c}$ , we have  $\vec{c} = A\vec{p}$ . If we have  $N$  pairs of  $\vec{p}$  and  $\vec{c}$ , then  $C = AP$ , where  $C = [\vec{c}_1, \vec{c}_2, \dots, \vec{c}_N]$ , and  $P = [\vec{p}_1, \vec{p}_2, \dots, \vec{p}_N]$  are both  $3 \times N$  matrices. The least square solution to  $A$  is  $A = C(P^T PP^T)^{-1}$ .

The 27 solid color images shown in Fig. 10 are used to estimate the camera's response matrix  $A$  to the projector's input. They are uniformly sampled in the RGB color space.

We project the same solid color image from both projectors at the same time, and capture it with the camera under the same settings as used for camera gray balancing. Then the same  $50 \times 55$  image patch as used in camera gray balancing is used. After we gray balance the camera's raw output, the least square solution to matrix  $A$  is calculated to estimate the camera's response to the projector. The result we got is

$$A = \begin{pmatrix} 0.418 & 0.022 & -0.016 \\ 0.031 & 0.381 & 0.010 \\ 0.017 & 0.143 & 0.263 \end{pmatrix}.$$

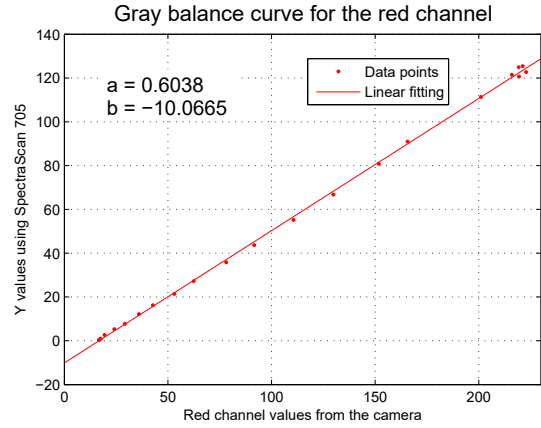
Note that the element at row 1 column 3 of our estimate for  $A$  is negative. This should not happen in a real imaging system. The reason we get negative element is that the system is not completely linear. We will leave it this way since the negative value is very close to 0.

### System Noise Characterization

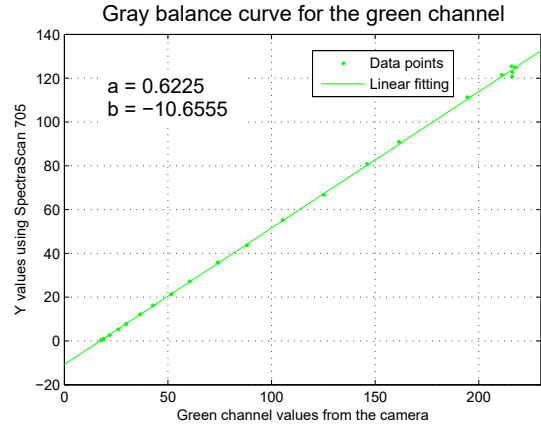
The images shown in Fig. 10 and the data captured for the previous subsection are used for noise characterization, as well. First, camera gray balancing is performed, then the same image patches used for the system color characterization are used here.

Assuming the imaging system is subject to additive zero-mean multivariate Gaussian noise, the noise covariance matrices  $\Sigma = [\sigma_{kl}^2]$  for the 27 measured colors are calculated separately. Each element of the covariance matrix is calculated as in Eq. 9.

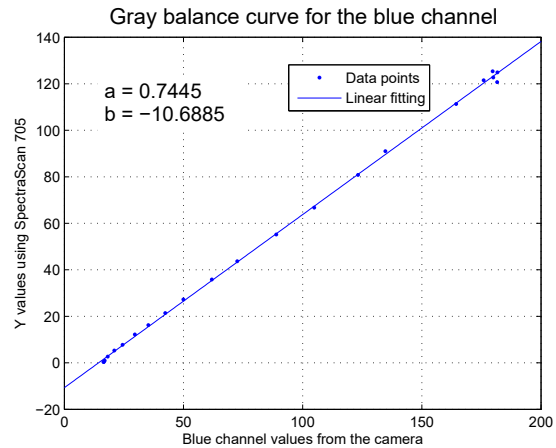
$$\sigma_{kl}^2 = \frac{1}{MN} \sum_{m=0}^{M-1} \sum_{n=0}^{N-1} (c_k[m, n] - \mu_k)(c_l[m, n] - \mu_l), k, l = R, G, B, \quad (9)$$



(a) Gray balance curve for the camera red channel.



(b) Gray balance curve for the camera green channel.



(c) Gray balance curve for the camera blue channel.

Figure 8: Camera gray balancing curves.

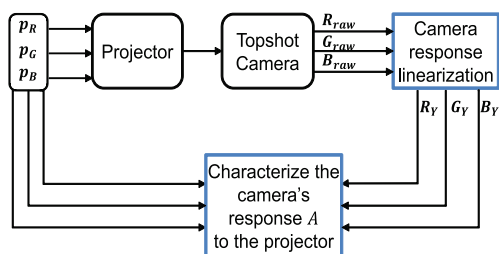


Figure 9: Block diagram for measuring the camera's response matrix to the projector's input.

where

$$\mu_k = \frac{1}{MN} \sum_{m=0}^{M-1} \sum_{n=0}^{N-1} c_k[m, n], k = R, G, B. \quad (10)$$

Here,  $M$ ,  $N$  are the number of rows and columns of the image patch we used, respectively. In practice, we use  $M = 50$  and  $N = 55$ .

From the measurement data, we get the noise covariance matrices for the 27 uniformly sampled data points in the projector's input RGB space. For colors other than the 27 we measured, trilinear interpolation is used to calculate each element of their corresponding noise covariance matrices. Sampled at points 0, 128, and 255 of each dimension, the 27 data points partition the projector's RGB space into 8 cubes, as shown in Fig. 11. Given a query color, it can be determined with a simple comparison at each dimension to which cube the query color belongs among the eight options. Each of the nine elements of its  $3 \times 3$  noise covariance matrix is computed by trilinear interpolation of the eight data points that form the cube to which it belongs. Figure 12 illustrates the concept of trilinear interpolation.

Let the coordinates of the unknown data point in the middle of the cube be  $(x_p, y_p, z_p)$ , and the coordinates of the eight vertices be  $(x_0, y_0, z_0)$ ,  $(x_0, y_0, z_1)$ ,  $(x_0, y_1, z_0)$ ,  $(x_0, y_1, z_1)$ ,  $(x_1, y_0, z_0)$ ,  $(x_1, y_0, z_1)$ ,  $(x_1, y_1, z_0)$ , and  $(x_1, y_1, z_1)$ . The value  $p$  at the point  $(x_p, y_p, z_p)$  can be calculated by the eight value of the vertices  $p_{000}$ ,  $p_{001}$ ,  $p_{010}$ ,  $p_{011}$ ,  $p_{100}$ ,  $p_{101}$ ,  $p_{110}$ , and  $p_{111}$  according to Eq. 11.

$$\begin{aligned} p = & p_{000}(1 - \Delta x)(1 - \Delta y)(1 - \Delta z) + p_{001}(1 - \Delta x)(1 - \Delta y)\Delta z \\ & + p_{010}(1 - \Delta x)\Delta y(1 - \Delta z) + p_{011}(1 - \Delta x)\Delta y\Delta z \\ & + p_{100}\Delta x(1 - \Delta y)(1 - \Delta z) + p_{101}\Delta x(1 - \Delta y)\Delta z \\ & + p_{110}\Delta x\Delta y(1 - \Delta z) + p_{111}\Delta x\Delta y\Delta z, \end{aligned} \quad (11)$$

where

$$\Delta x = \frac{x_p - x_0}{x_1 - x_0}, \Delta y = \frac{y_p - y_0}{y_1 - y_0}, \Delta z = \frac{z_p - z_0}{z_1 - z_0}. \quad (12)$$

### Optimal Projector Input Colors

In the previous section, we have measured the system color and noise characteristics. The remaining unknowns are the projectors' inputs  $\bar{p}_1$ , and  $\bar{p}_2$ . In this section, we define an optimization problem to determine the best input colors for the projectors

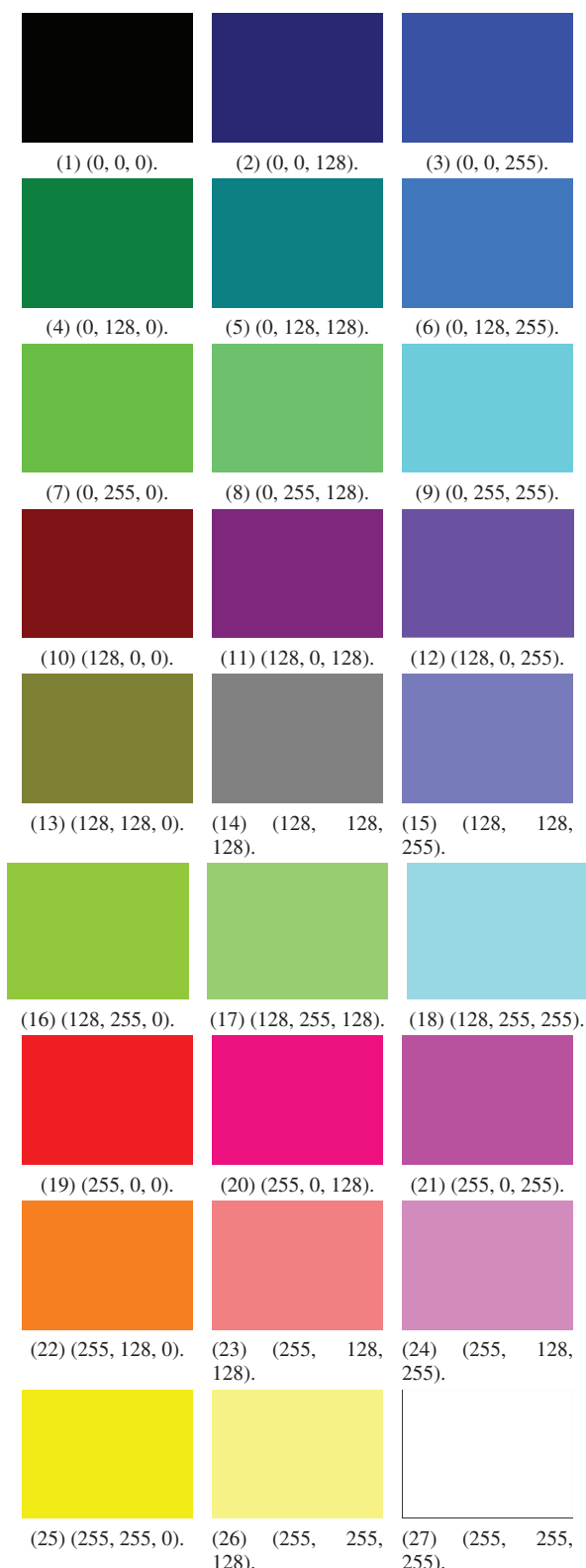


Figure 10: Different solid color images used for system color and noise characterization. The red, green, and blue channel values for each color are labeled under the corresponding image.



in the same dimension is set to be 2, in order to reduce the computation.

The integration region  $\Omega_j$  represents that a point in this region would lead to a decision of  $o = j$  among all the possible four outcomes. We use the maximum likelihood method to determine the integration region. Taking the logarithm of the multivariate Gaussian probability density function, we have

$$\ln f(\vec{x}; \vec{\mu}, \Sigma) = -\frac{n}{2} \ln(2\pi) - \frac{1}{2} \ln |\Sigma| - \frac{1}{2} (\vec{x} - \vec{\mu})^T \Sigma^{-1} (\vec{x} - \vec{\mu}). \quad (20)$$

Define

$$g_i(\vec{x}) = -\frac{1}{2} (\vec{x} - \vec{\mu}_i)^T \Sigma_i^{-1} (\vec{x} - \vec{\mu}_i) - \frac{1}{2} \ln |\Sigma|_i, \quad (21)$$

where  $i = 0, \dots, 3$ .

For each sample point  $\vec{x}_0$ , when making the decision we compute  $g_i(\vec{x}_0)$ ,  $i = 0, \dots, 3$ , and find

$$K = \arg \max_i (g_i(\vec{x}_0)). \quad (22)$$

Then this sample point  $\vec{x}_0$  falls into the integration region  $\Omega_K$ . For example, if there are only two possible outcomes  $\vec{c}_0$  and  $\vec{c}_1$ ,

$$\vec{x}_0 \in \Omega_0 \Leftrightarrow g_0(\vec{x}_0) \geq g_1(\vec{x}_0). \quad (23)$$

### The Optimal Solution

When searching for optimal solutions, we magnify all the noise covariance matrices that are measured by a factor of 25 to make the difference of the cost function larger for the different variables.

We generated 100 random starting points based on a uniform distribution between  $[0, 0, 0]^T$  and  $[255, 255, 255]^T$ . The smallest cost function value we obtained after running the pattern search method on all starting points was  $2.89 \times 10^{-6}$ . The corresponding optimal solution is shown in Eq. 24.

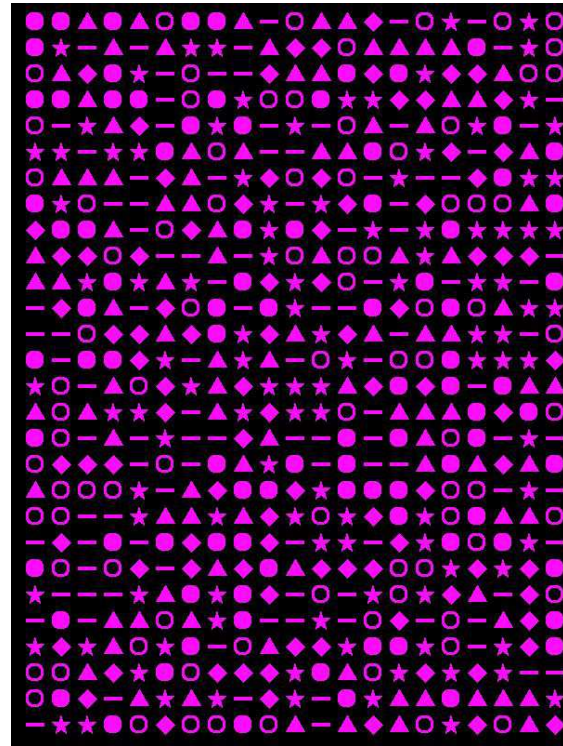
$$\hat{p}_1 = \begin{pmatrix} 255 \\ 13 \\ 255 \end{pmatrix}, \hat{p}_2 = \begin{pmatrix} 8 \\ 255 \\ 255 \end{pmatrix}. \quad (24)$$

The corresponding colored M-array patterns are shown in Fig. 13.

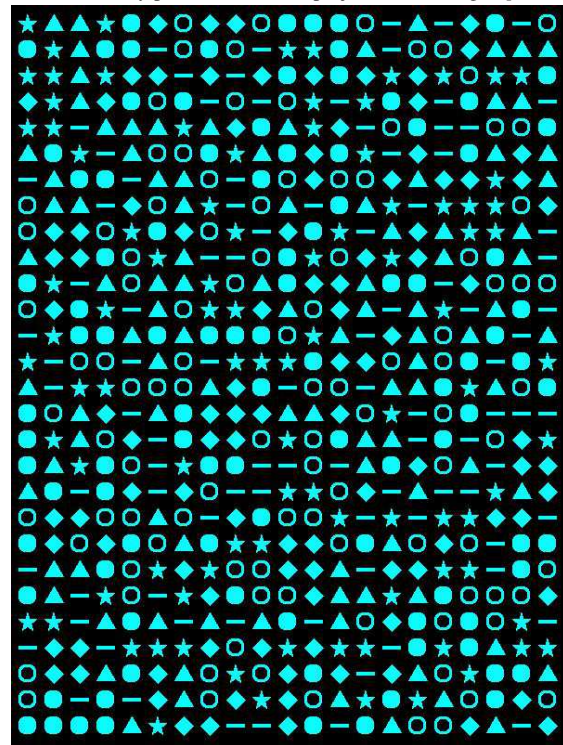
### Validation of the System Model

After getting the optimal solution from the pattern search method, we recommend to calculate its classification accuracy for each of the four classes. The result can also be examined visually. The maximum likelihood decision method should be used as defined in the system model.

In practice, we should generate the two M-array patterns with corresponding colors, and project them from two projectors at the same time. The camera's exposure setting should be adjusted according to the two new colors, so that fewer than 1 percent of the pixels are saturated for each red, green, and blue channel. In the exposure adjustment, two solid new color patterns should be projected. Since the exposure adjustment is a linear process, it will not change the characteristics of the imaging system. Then we capture an image of the M-array patterns with the camera's new exposure setting.



(a) M-array pattern for the left projector according to  $\hat{p}_1$ .



(b) M-array pattern for the right projector according to  $\hat{p}_2$ .

Figure 13: M-array pattern for the two projectors according to the optimal solution  $\hat{p}_1, \hat{p}_2$ .

For each pixel, we take its camera RGB value and gray balance them first. On the other hand, the ideal value for each case  $\bar{c}_i, i = 0, \dots, 3$ , is obtained by  $A\bar{p}$ . The maximum likelihood method is then used to compare the actual  $\bar{c}$  and nominal  $\bar{c}_i$  to make the decision.

To validate the solution to the optimization problem, we can compare the optimal solution with a naive solution. For example, using red and green for the projectors' inputs. Under this condition, the cost function value is  $5.00 \times 10^{-4}$ .

$$\bar{p}_{1,naive} = \begin{pmatrix} 255 \\ 0 \\ 0 \end{pmatrix}, \bar{p}_{2,naive} = \begin{pmatrix} 0 \\ 255 \\ 0 \end{pmatrix}. \quad (25)$$

## Conclusions

In this paper, we propose a color multiplexed camera-projector imaging system model, and perform the spectral analysis for it. The system color and noise characterization processes and results are described as well. The characterization results provide parameters for the color multiplexed system model. An optimization problem is defined to determine the best input colors for the system. The optimal solution we get from 100 different starting points for the pattern search method is presented. A procedure to validate a solution to the optimization problem is described at the end.

This color multiplexed system model is not limited to our imaging system, and can be applied to other multichannel problem as well.

There are more things we can do to make the system more accurate. First of all, we use the overlapped region of the two projectors to characterize the imaging system. But the two projectors are not exactly the same. It might be better to characterize the two projectors and the overlapped region separately. Secondly, the noise is assumed to be the same across the camera's field of view. Further measurements can be done to characterize the spatial dependence of the noise.

## References

- [1] J. Allebach. *Notes for ECE 638: Principles of Digital Color Imaging Systems*, 2017. <http://engineering.purdue.edu/~ece638/>.
- [2] F. Cheng, C. Lu, and Y. Huang. 3D object scanning system by coded structured light. In *3rd International Symposium on Electronic Commerce and Security (ISECS)*, pages 213–217, 2010.
- [3] Y. Cui, S. Schuon, D. Chan, and S. Thrun and C. Theobalt. 3D shape scanning with a time-of-flight camera. In *Proceedings of the IEEE Computer Society Conference on Computer Vision and Pattern Recognition*, pages 1173–1180, 2010.
- [4] J. Dong, K. R. Bengtson, B. Robinson, and J. P. Allebach. Low-cost structured-light 3D capture system design. In *Three-Dimensional Image Processing, Measurement (3DIPM), and Applications, SPIE Vol. 9013*, March 2014.
- [5] Robert Hooke and T. A. Jeeves. "Direct Search" solution of numerical and statistical problems. *J. ACM*, 8(2):212–229, April 1961.
- [6] D. Lanman and G. Taubin. Build your own 3D scanner: 3D photography for beginners. In *ACM SIGGRAPH 2009 Courses*, 2009.

- [7] Yang Lei, K.R. Bengtson, L. Li, and J.P. Allebach. Design and decoding of an m-array pattern for low-cost structured light 3D reconstruction systems. In *2013 IEEE International Conference on Image Processing (ICIP)*, pages 2168–2172, Sept 2013.
- [8] C. T. Wu, K. R. Bengtson, and J. P. Allebach. Captured open book image de-warping using depth information. In *2015 IEEE International Conference on Image Processing (ICIP)*, pages 197–201, Sept 2015.

## Author Biography

**Yang Lei** received her BS in Electrical Engineering from Sichuan University (2009) and her PhD in Electrical Engineering from Purdue University (2014). Since then she has worked at HP Labs in Palo Alto, CA. Her work has focused on 3D imaging systems and applications in object recognition and tracking.

**Jan P. Allebach** is Hewlett-Packard Distinguished Professor of Electrical and Computer Engineering at Purdue University. Allebach is a Fellow of the IEEE, the National Academy of Inventors, the Society for Imaging Science and Technology (IS&T), and SPIE. He was named Electronic Imaging Scientist of the year by IS&T and SPIE, and was named Honorary Member of IS&T, the highest award that IS&T bestows. He has received the IEEE Daniel E. Noble Award, and the OSA/IS&T Edwin Land Medal. He is a member of the National Academy of Engineering.